ACS APPLIED MATERIALS & INTERFACES
Research Article
www.acsami.org

Mesoporous Organosilica with Amidoxime Groups for CO_2 Sorption

Chamila Gunathilake and Mietek Jaroniec*

Department of Chemistry and Biochemistry, Kent State University, Kent, Ohio 44242, United States

Supporting Information

ABSTRACT: Incorporation of basic species such as amine-containing groups into porous materials is a well-established strategy for achieving high uptake of acidic molecules such as CO_2. This work reports a successful use of the aforementioned strategy for the development of ordered mesoporous organosilica (OMO) with amidoxime groups for CO_2 sorption. These materials were prepared by two-step process involving: (1) synthesis of OMO with cyanopropyl groups by co-condensation of (3-cyanopropyl)triethoxysilane and tetraethylorthosilicate in the presence of Pluronic P123 triblock copolymer under acidic conditions, and (2) conversion of cyanopropyl groups into amidoxime upon treatment with hydroxylamine hydrochloride under suitable conditions. The resulting series of amidoxime-containing OMO was prepared and used for CO_2 sorption at low (25 °C) and elevated (60, 120 °C) temperatures. These sorbents exhibited relatively high adsorption capacity at ambient conditions (25 °C, 1 atm) and remarkable high sorption uptake (∼3 mmol/g) at 60 and 120 °C. This high CO_2 uptake at elevated temperatures by amidoxime-containing OMO sorbent makes it a noticeable material for CO_2 capture.

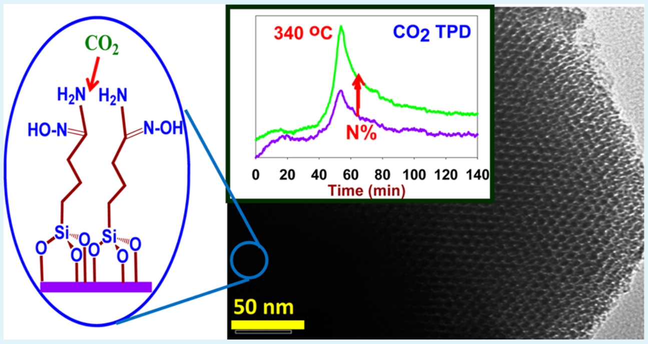

KEYWORDS: *CO_2 sorption, amidoxime functionality, temperature-programmed desorption, ordered organosilica mesostructures*

INTRODUCTION

Nowadays, global climate change has attracted a significant attention worldwide. Continuous increment of CO_2 concentration is mainly caused by fossil fuels-based power plants, which are the largest source of CO_2 discharge into atmosphere. Chemical, petrochemical, iron, steel, and cement industries, and automobiles are the other sources of CO_2. According to EPA (USA), such greenhouse gas emissions can cause a rise in temperature by 2−4 °C during the next century, if the atmospheric levels of CO_2 are not reduced. Although this change may be considered to be small, it could lead to catastrophic consequences for our planet in the long time scale. Thus, it is very important to diminish the excessive CO_2 concentration in atmosphere. So far, a variety of methods has been applied to mitigate the effect of greenhouse gases. The existing technology for large scale CO_2 capture utilizes liquid amine scrubbing by using aqueous solutions of MEA (monoethanolamine), DEA (diethanolamine), diglycolamine, and their derivatives such as *N*-methyldiethanolamine. Acidic CO_2 chemically reacts with the aforementioned basic amines removing up to 3−4 mmol of CO_2 per gram of amine. The captured CO_2 is regenerated by heating the mixture above 100 °C.[1] The regenerated CO_2 is then compressed and transported for various industrial utilizations such as urea production, beverage industry, oil recovery, and dry ice production.[2] However, there are numerous drawbacks of the liquid amine scrubbing process such as high energy consumption needed for regeneration of CO_2 and relatively low thermal stability of liquid amines. In addition, this method produces corrosive products, subjected to oxidative degradation, shows lower selectivity for CO_2 in the presence of other gases such as SO_2, NO_2, and NO, and smaller chemical stability and tolerance to impurities.

The aforementioned drawbacks can be significantly diminished by using solid sorbents for CO_2 capture. Among various sorbents the amine-modified porous materials have been extensively explored. These sorbents are often prepared by physical impregnation of porous solids with monomeric or polymeric amines or by chemical incorporation of amine-containing functionalities into porous mesostructures. The latter can be achieved by one-pot co-condensation synthesis of porous solids such as silica in the presence of amine-containing silanes or by postsynthesis grafting. The aforementioned co-condensation method is simpler, and less time-consuming. High loading of organic functionalities and adjustable structure formation are additional advantages of this strategy. Also, the co-condensation creates better opportunities for tailoring the framework and surface properties by using one or more functional organosilanes to obtain materials with good structural ordering, accessible porosity, high surface area, and high content of amine-containing groups. There are numerous reports showing advantages of the co-condensation method over other methods used for the synthesis of amine-containing ordered siliceous mesostructures.[3−6]

Received: May 14, 2014
Accepted: July 3, 2014
Published: July 3, 2014

dx.doi.org/10.1021/am5028742 | *ACS Appl. Mater. Interfaces* 2014, 6, 13069−13078

3-Aminopropyltriethoxysilane[$NH_2(CH_2)_3Si(OC_2H_5)_3$; AP], N-[3-(trimethoxysilyl)propyl] ethylenediamine [$NH_2(CH_2)_2NH\ (CH_2)_3Si(OCH_3)_3$; DA], (3-trimethoxysilylpropyl)diethylenetriamine [$NH_2(CH_2)_2NH(CH_2)_2NH(CH_2)_3Si(OCH_3)_3$; TA], and some of their derivatives are most often used to synthesize amine-functionalized mesoporous organosilica materials for CO_2 capture. The resulting mesoporous organosilica materials with incorporated amine-containing functionalities possess high surface area, accessible porosity, and large amount of nitrogen groups showing high affinity toward CO_2 molecules. For instance, Canck et al.[7] studied periodic mesoporous organosilicas with various dangling groups containing $-NH_2$ and $-NH-$ for CO_2 adsorption. It was shown that organosilicas with diaminododecane functionality appear to be good materials for CO_2 chemisorption under dry conditions. Knowles and co-workers[8−10] showed that amine functionalization of silica depends on its surface properties, specific surface area, pore geometry, pore volume, concentration of silanols, and modification conditions. These authors further demonstrated that the higher nitrogen content in the silica sorbent resulted in higher CO_2 sorption capacity. They reported about 1.7 mmol/g sorption capacity in flowing 90% CO_2 and 10% Ar gases at 20 °C. Hiyoshi and co-workers studied SBA-15 mesoporous silica grafted with the aforementioned AP, DA, and TA aminosilanes.[11] It was shown that the CO_2 adsorption capacity of these materials increased with the number of amine groups in the attached ligands. At the same nitrogen content, CO_2 adsorption changed according to the following order: AP > DA > TA. This finding was also confirmed by Zelenak et al.[12] for amine-modified MCM-41, SBA-15, and SBA-12 silica substrates. Harlick and Sayari showed that high adsorption capacity can be achieved for ordered mesoporous silicas with expanded pores because they can accommodate large quantity of amino groups.[13] However, the degradation of amine groups is a significant issue in CO_2 adsorption processes because it causes economic, operational, and environmental problems. In the case of the common sorbents, obtained by using AP, DA, TA, and MEA organosilanes, the aforementioned degradation would require the replacement of more than 2.0 kg of amines per one tone of the captured CO_2, leading to an increase of the operation cost.[14] A comprehensive study of the stability of amine groups was done by Sayari and co-workers for a wide variety of mesoporous silica-based sorbents; it was found that amine groups, including primary and secondary monoamines, mixed primary and secondary di- and triamines as well as different polyethylenimines, start to decompose above 100 °C.[15−17] Oxidative degradation is another significant drawback of amine groups, caused mainly by dissolved oxygen. This type of degradation often occurs during CO_2 capture from flue gases containing high O_2 content (∼5%).[18] To mitigate the O_2 content, several methods such as the addition of O_2 scavengers, reaction inhibitors, and chelating agents have been proposed. Degradation of amine groups is also possible during thermal regeneration process at high temperatures.[19] The aforementioned literature survey shows the importance of thermally stable sorbents for CO_2 capture and outlines the existing challenges. While the synthesis of various amine-containing siliceous sorbents has been achieved, there is still a room for improvement of their composition, structure, morphology, and thermal stability during the CO_2 capture and sorbent regeneration processes. The aforementioned limitations of amine-containing siliceous sorbents provided inspiration for the current study.

Here we explore the use of amidoxime-containing sorbents for CO_2 capture at flue gas conditions. Recently Zulfiqar and co-workers[20] reported the use of amidoxime compounds for CO_2 capture at high pressures (∼180 bar) and elevated temperatures (43 and 70 °C). By taking the binding energy between CO_2 and amidoxime into account, these authors concluded that the planar structure of amidoxime is able to bind CO_2 via amine and hydroxyl functional groups simultaneously, whereas in the case of MEA, CO_2 preferentially interacts with hydroxyl group alone in the lowest energy state. Later, Mahurin and co-workers grafted porous carbons with amidoxime groups and measured the CO_2 uptake at 0 and 25 °C;[21] it was shown that at the aforementioned temperatures the resulting amidoxime-modified carbons adsorbed less of CO_2 than pristine activated carbons, which was related to the surface area reduction caused by grafting. Patel and co-workers synthesized amidoxime-containing polymeric sorbents with intrinsic microporosity and observed an increase in the CO_2 uptake at 25 °C with increasing amount of amidoxime loading.[22]

Nonsiliceous inorganic sorbents have been also widely studied for the CO_2 capture in the past decade. For instance, interaction of carbon dioxide with the surface of zirconium oxide was investigated by Bachiller group.[23] They showed that the crystallographic nature of ZrO_2 significantly determines the structure formation between CO_2 and the ZrO_2 surface, its chemical stability, and the number of CO_2 sorption sites available on the ZrO_2 surface. The FTIR spectroscopy was used to explain interaction of CO_2 with the ZrO_2 surface and to determine the basic sites on this surface for CO_2 sorption.[23−25] Notably, the synthesis of mesoporous zirconia-silica composite showed better structural parameters such as the pore volume, microporosity, 3D interconnected mesoporosity, and specific surface area. This composite material displayed high thermal and mechanical stability, resistivity to corrosion, and relatively high affinity toward CO_2 molecules.

In this study, (3-cyanopropyl)triethoxysilane (CPS) and tetraethylorthosilicate (TEOS) were used as silica precursors to obtain ordered mesoporous organosilica (OMO) with cyanopropyl groups. Next, the aforementioned cyanopropyl groups were converted to amidoxime groups ($-C{=}N(NH_2)$-OH) using hydroxylamine hydrochloride ($NH_2OH.HCl$) under suitable synthesis conditions[26] (see Figure S1 in the Supporting Information). Note that porous materials with amidoxime groups have been applied for uranium adsorption and showed high uranium uptake and rapid adsorption kinetics.[26−30] The aforementioned OMO with cyanopropyl groups was synthesized using the procedure reported in ref 31 for synthesis of SBA-15; TEOS was used to increase cross-linking and obtain highly ordered organosilica. An environmentally friendly, cheep, and biodegradable triblock copolymer (Pluronic P123) was used as a soft template. In addition, some composite samples consisting of OMO with amidoxime groups and zirconia (as a nonsiliceous inorganic sorbent) were prepared to explore the effect of zirconia on the sorbent stability and CO_2 uptake. All synthesized materials were tested for CO_2 sorption at ambient pressures (up to ∼1 atm) and temperatures of 25, 60, and 120 °C. The resulting amidoxime-containing OMO materials showed very good structural parameters such as the specific surface area, porosity, and excellent thermal stability during sorption process. To the best of our knowledge, this is the first attempt to synthesize a series of silica-based materials with amidoxime groups and zirconia for CO_2 capture at ambient and elevated temperatures.

EXPERIMENTAL SECTION

Materials. (3-Cyanopropyl)triethoxysilane(CPS) was purchased from Alfa Aesar, Johnson Matthey Company, Ward Hill, Massachusetts. Hydroxylamine hydrochloride ($NH_2OH.HCl$) was purchased from Sigma-Aldrich. Pluronic P123 ($EO_{20}PO_{70}EO_{20}$) triblock copolymer was donated by BASF Corporation, Florham Park, NJ; 95% ethanol, 36% HCl, and NaOH were purchased from Fisher Scientific, Pittsburgh, PA; tetraethylorthosilicate (TEOS) was purchased from Gelest Inc., Morrisville, PA; zirconyl chloride octahydrate ($ZrOCl_2\cdot 8H_2O$) was purchased from Acros Organic, NJ. Deionized water (DW) was obtained using in house Ion pure Plus 150 Service Deionization ion-exchange purification system. All reagents were analytical grade and used without further purification.

Preparation. The recipe used for preparation of OMO with cyanopropyl groups was reported elsewhere[31] for the synthesis of SBA-15. In general, triblock copolymer P123 (2 g) was mixed with 2 M HCl (61.2 mL) and distilled water (10.8 mL). P123 was completely dissolved within 3.5 h under rapid stirring at 40 °C. After 3.5 h, the predetermined amount of CPS (10, 20, 40%) was added to the mixture. Half an hour later, 4.43 cm^3 (0.02 mmol) of TEOS was added dropwise to the P123-HCl-DW mixture under rapid stirring at 40 °C. The resultant mixture was further stirred for 24 h and aged at 100 °C. The powder was filtered and washed with 2 M HCl and dried overnight at 80 °C. The polymeric template was removed by extraction using 1g of the as synthesized material with 2 mL of 36% HCl and 100 mL of 95% ethanol at 70 °C for 24 h and dried overnight in oven at 100 °C. The amidoximation reaction (see Figure S1 in the Supporting Information) was performed using 16.6% (w/v) hydroxylamine solution in a 50/50 solution H_2O/MeOH at pH 8 for 16 h at 70 °C in a reflux condenser. The product was then washed with DW. Notation of the samples starts with CP referring to OMO with cyanopropyl groups followed by the percentage of the organosilane used in the synthesis mixture. The molar percentage of organosilane was calculated as follows: X % = [moles of CPS × 100]/ [moles of (CPS + TEOS)]. The number (0.02) of moles of TEOS was kept constant during synthesis. All extracted samples are denoted with asterisk mark (*). Samples with (#) represent the as-synthesized ones. CP-X*-AO refers to the extracted samples with cyanopropyl groups converted to amidoxime (AO) groups using hydroxylamine hydrochloride. For instance, CP-40*-AO refers to the sample obtained by using 40% of CPS, extracted with acidic ethanol and reacted with $NH_2OH.HCl$ to convert cyanopropyl groups to amidoxime ones.

Additional samples were obtained by using 0.005 mol of zirconyl chloride octahydrate as zirconia precursor to the aforementioned reaction mixture. These samples were also subjected to extraction followed by amidoximation and labeled as Zr-CP-X*-AO. All amidoxime-containing samples were also subjected to pretreatment (heating up to 350 °C in helium) before pulse chemisorption and TPD (temperature-programmed desorption) measurements. These samples are labeled as CP-X*-AO−CO_2 (where X = 10, 20, 40).

Characterization. Nitrogen adsorption isotherms were measured at −196 °C on an ASAP 2010 volumetric analyzer (Micromeritics, Inc., Norcross, GA). Prior to adsorption measurements, all samples were outgassed under vacuum at 110 °C for 2 h. Powder X-ray diffraction (XRD) measurements were performed using an X'Pert PRO MPD multipurpose diffractometer (PANalytical, Inc.) with Cu Kα radiation (0.15406 nm) at room temperature from 0.4 to 5.0° (small angle). Measurements were conducted using a voltage of 45 kV, a current setting of 40 mA, a step size of 0.02°, and count times of 20 s (small angle). Microscope glass slides were used as sample supports for all samples.

High resolution thermogravimetric measurements were recorded on TGA Q-500 analyzer (TA Instruments, Inc., New Castle, DE). Thermogravimetric (TG) profiles were recorded from 25 to 700 °C in flowing nitrogen with a heating rate of 10 °C/min using a high resolution mode. The weight of each analyzed sample was typically in 5−20 mg range. The TG profiles were used to obtain information about the extent of the template removal.

Quantitative estimation of organic groups and N (%) was obtained by CHNS analysis using a LECO model CHNS-932 elemental analyzer (St. Joseph, MI). $^1H-^{13}C$ cross-polarization (CP) MAS NMR spectra were recorded using Bruker Avance (III) 400WB NMR spectrometer (Bruker Biospin Corporation, Billerica, MA, USA) with MAS triple resonance probe head using zirconia rotors 4 mm in diameter. $^1H-^{13}C$ CP-MAS NMR spectra were acquired at 400.13 MHz for ^1H and 100.63 MHz for ^{13}C. The MAS rate was 5 kHz. ^1H $\pi/2$ pulse length was 3.5 μs and pulse delay 2.0 s. TPPM20 ^1H decoupling sequence was used during acquisition. The ^{13}C chemical shifts were referenced to p-dioxane 66.6 ppm.

Transmission electron microscopy (TEM) images were obtained on a FEI Tecnai G2 F20 microscope. Prior to TEM analysis, the sample powders were dispersed in ethanol by moderate sonication at concentrations of ∼5 wt %. A lacey carbon-coated, 200-mesh, copper TEM grid was dipped into the sample suspension and then dried under vacuum at 80 °C for 12 h.

Room-Temperature CO_2 Adsorption Measurements. CO_2 adsorption on the selected cyanopropyl- and amidoxime-containing mesoporous materials was measured in the pressure range up to 1 atm on ASAP 2020 volumetric adsorption analyzer (Micromeritics, Inc., GA) at 25 °C using ultrahigh purity (99.99%) gaseous CO_2. Prior to adsorption analysis each sample was outgassed at 110 °C for 2 h under vacuum.

CO_2 Chemisorption and TPD Measurements. CO_2 chemisorption and TPD experiments were conducted using a Micromeritics Auto Chem II Chemisorption Analyzer (Micromeritics, Inc., GA) equipped with a thermocouple detector (TCD). Approximately 50−100 mg of each sample were loaded in a quartz tube microreactor supported by quartz wool and subjected to pretreatment at 350 °C for 10 min before CO_2 sorption, using a heating rate of 10 °C/min in flowing helium (at a rate of 50 cm^3/min). Next, the sample was cooled to selected temperature (120/60 °C) using heating rate of 10 °C/min, exposed to pulse of 5% CO_2−He (50 cm^3/min) as a loop gas, kept for 3 min, and allowed for return to baseline. Recording was repeated until peaks are equal or 30 times. Recording was taken every 0.1 s and finally post CO_2 pulse purge was applied in flowing helium (50 cm^3/min) for 30 min. In the TPD experiments, the samples were heated up to 350 °C using a heating rate of 5 °C/min and kept at this temperature for 90 min. The amounts of desorbed CO_2 were obtained by integration of the desorption profiles and referenced to the TCD signals calibrated for known volumes of analyzed gases.

Calculations. The Brunauer−Emmett−Teller specific surface areas (S_{BET}) were calculated from the N_2 adsorption isotherms in the relative pressure range of 0.05−0.2 using a cross sectional area of 0.162 nm^2 per nitrogen molecule. The single-point pore volume (V_{sp}) was estimated from the amount adsorbed at a relative pressure (p/p^0) of ∼0.98. The pore size distributions (PSD) were calculated using adsorption branches of nitrogen adsorption−desorption isotherms by the improved KJS method calibrated for cylindrical pores.[32] The pore width (W_{max}) was obtained at the maximum of the PSD curve.

RESULTS AND DISCUSSION

Properties of Cyanopropyl- and Amidoxime-Containing Samples.

Removal of the template from as-synthesized organosilica mesostructures with cyanopropyl groups, conversion of these groups to amidoxime functionalities via reaction with hydroxylamine hydrochloride, and thermal stability of amidoxime-containing samples upon CO_2 uptake were monitored by high-resolution thermogravimetry. The differential TG (DTG) and TG profiles are displayed in Figure 1 and Figure S2 in the Supporting Information, respectively. The DTG profile for the extracted sample (CP-X*, X = 10, 20, 40) shows three important thermal events (see for instance, the DTG curve for CP-20* in Figure 1). Thermal events at the

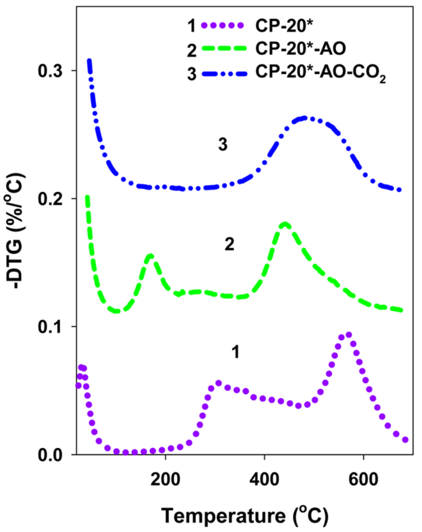

Figure 1. DTG curves for the extracted (CP-20*) cyanopropyl-containing organosilica mesostructures, and for amidoxime-containing samples without (CP-20*-AO) and with (CP-20*-AO- CO_2) chemisorbed CO_2.

temperature range of 25−110 °C correspond to the evaporation of physically adsorbed water and possibly solvent. The second peak in the range of 250−360 °C, although much smaller as that observed for as-synthesized samples (not shown here), indicates that P123 block copolymer template was not completely removed via extraction. The third event occurred at 570 °C represents the decomposition of cyanopropyl groups present in OMO.

The DTG profile obtained for amidoxime-containing OMO sample, CP-20*-AO, exhibits two peaks at the temperature ranges of 140−230 and 400−500 °C (see the DTG curve in Figure 1). The first one accounts for desorption of adsorbed water/solvent. The second peak located at 450 °C is obviously related to the decomposition of amidoxime groups; in this temperature range dehydroxylation of the surface OH groups occurs too and contributes to the observed thermal event. The shift of the last peak observed on the DTG profile for CP-20* from 570 to 450 °C in the case of CP-20*-AO provides evidence about successful conversion of cyanopropyl groups to amidoxime functionalities. The DTG curve for the CP-20*-AO sample with chemisorbed CO_2 (CP-20*-AO−CO_2) is also displayed in Figure 1. As can be seen from this figure, the peak centered at 450 °C is again shifted to 500 °C and much broader upon CO_2 adsorption. The corresponding TG curves for these samples are shown in Figure S2 in the Supporting Information. A comparison of the DTG peaks at ∼570 °C (Figure 2) for CP-20* and CP-40* samples shows an increase of the peak intensity for the latter sample due to higher loading of cyanopropyl groups. An analogous behavior is observed for the DTG peaks at ∼450 °C obtained for CP-20*-AO and CP-40*-AO samples (Figure 2) as well as for the DTG peaks obtained for these samples with chemisorbed CO_2 at 120 °C (CP-20*-AO−CO_2 and CP-40*-AO−CO_2). The corresponding TG curves for these samples are also shown in Figure S3 in the Supporting Information. It is noteworthy that the slightly lower thermal stability of CP-40* in relation to CP-20* is expected because an increase in the loading of organic groups in siliceous frameworks make these mesostructures more prone to thermal degradation.

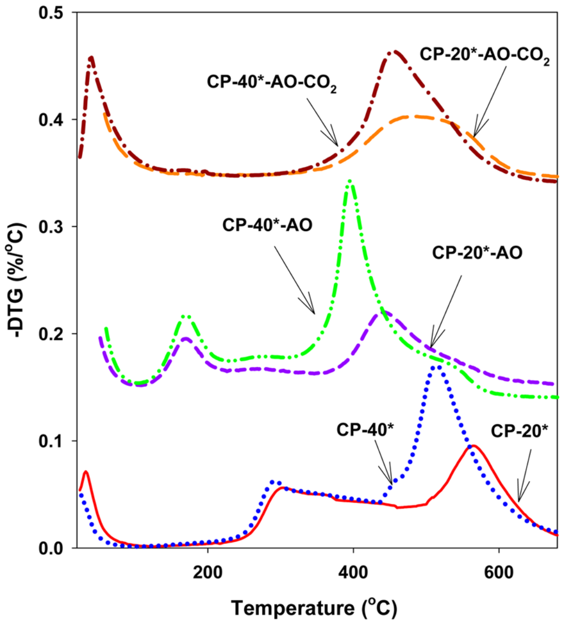

Figure 2. A comparison of the DTG curves for the extracted cyanopropyl-containing organosilica mesostructures before (CP-*X**) and after amidoximation (CP-*X**-AO; *X* = 20 and 40% of CPS in the synthesis mixture) as well as for two samples with different concentration of amidoxime groups after CO_2 chemisorption (top curves).

The TG and DTG profiles recorded for the Zr-CP-20* and Zr-CP-20*-AO samples are similar to those obtained for CP-20*, and CP-20*-AO, respectively (not shown here). Nitrogen content values for cyanopropyl and amidoxime-containing samples are summarized in Table 1. Nitrogen content for CP-40* is 4.35%, more than two times higher than that obtained for CP-20*. Amidoximation inevitably increased N (%) as expected because two N atoms are in amidoxime group =(−CH_2−CH_2−C(NH_2)=NOH) as compared to one N atom in cyanopropyl (−CH_2−CH_2−C≡N) group. According to the theoretical calculations based on N % about 70% of

Table 1. Adsorption and Structural Parameters for the Samples Studied

content	V_{sp} (cc/g)	V_{mi} (cc/g)	S_{BET} (m^2/g)	W_{max} nm	V_t (cc/g)	N %
CP-10*	0.80	0.10	698	7.61	0.84	1.30
CP-10*-AO	0.78	0.05	533	8.04	0.83	1.80
CP-20*	0.83	0.11	771	6.56	0.89	2.01
CP-20*-AO	0.65	0.05	500	7.16	0.69	2.65
CP-40*	0.34	0.05	363	4.90	0.36	4.35
CP-40*-AO	0.21	0.04	257	4.26	0.22	5.16
Zr-CP-20*	0.63	0.11	599	3.40	0.66	1.71
Zr-CP-20*-AO	0.60	0.08	585	2.95	0.61	2.27

V_{sp}-single-point pore volume calculated at the relative pressure of 0.98; V_{mi}—volume of fine pores (micropores and small mesopores below 3 nm) calculated by integration of the PSD curve up to 3 nm; S_{BET} − specific surface area calculated from adsorption data in relative pressure range 0.05−0.20; W_{max} - pore width calculated at the maximum of PSD obtained by using the improved KJS method;[32] V_t - total pore volume calculated by integration of the PSD curve; N % obtained by CHNS analysis.

cyanopropyl groups was converted to amidoxime groups in the samples studied.

$^{1}H-^{13}C$ CP/MAS NMR spectra confirmed the presence of $-CH_2-CH_2-C{\equiv}N$ and $-CH_2-CH_2-C(NH_2){=}NOH$ groups in organosilica mesostructures. ^{13}C CP/MAS NMR spectra for CP-20*, CP-40*, and CP-20*-AO samples are shown in Figure 3. Five intense resonance peaks visible at chemical shifts at 11.2, 18.30, 35.4, 59.5, and 118.9 ppm can be assigned to methylene carbon atom directly connected to silicon, to the unreacted methyl carbon in ethoxy group, to the methylene carbon atom linked to another carbon atom in methylene group, to the methylene carbon atoms of the nonhydrolyzed ethoxy group, and, finally to the nitrile carbon atom in the CP-20* and CP-40* samples.[33,34] Similar peaks at 11.1, 18.0, 35.3 59.5, 118.3 with one additional peak at 157.2 ppm are visible for CP-20*-AO sample.[33−36] This additional peak at 157.2 ppm confirms the conversion of nitrile group to amidoxime.[35,36] However, a less-intensive peak remaining at 118 ppm reveals the existence of a small amount unreacted cyanopropyl groups.

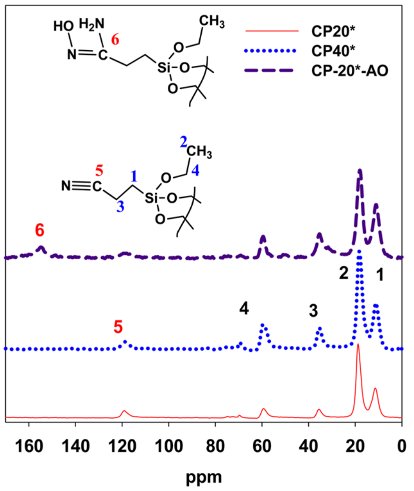

Figure 3. $^{1}H-^{13}C$-CP/MAS NMR spectra of extracted cyanopropyl-containing organosilica samples (CP-20*, CP-40*) and amidoxime-containing sample (CP-20*-AO).

Structural characterization of the mesoporous organosilica samples studied was performed by small-angle X-ray diffraction (XRD) in the range of 2θ from 0.5 to 2 degree. The XRD patterns of the as-synthesized (CP-20$^{\#}$), extracted (CP-20*), and amidoxime-modified (CP-20*-AO) samples are shown in Figure 4. As can be seen in this figure, the XRD pattern for the as-synthesized sample displays one major peak. Diffraction patterns for both extracted cyanopropyl- and amidoxime-containing organosilica samples also exhibit one sharp reflection peak at $2\theta \approx 0.85°$ indexed as 100 with two minor well-resolved reflection peaks indexed as 110 and 200 according to the *p6mm* symmetry group representing hexagonal channel-like mesostructure. The remaining CP-10*, CP-10*-AO, CP-40*, and CP-40*-AO samples were also studied by XRD (see Figure S4 in the Supporting Information). No significant deviation in relation to the intensity and location of the XRD peaks for CP-20* and CP-20*-AO is observed on the peaks recorded for CP-10* and CP-10*-AO samples. However, as can be seen from Figure S4 in the Supporting Information, an increase in the percentage of CPS in the reaction mixture led to a pronounced change in the XRD profiles, indicating that the structural order of the mesoporous organosilicas studied is apparently dependent on the loading of organic groups. For instance, the XRD patterns for the CP-40* and CP-40*-AO samples exhibit one peak at 2θ equal to 0.85 and 1.2°, respectively, indicating a significant deterioration of ordered mesostructures at high loadings of organic groups.

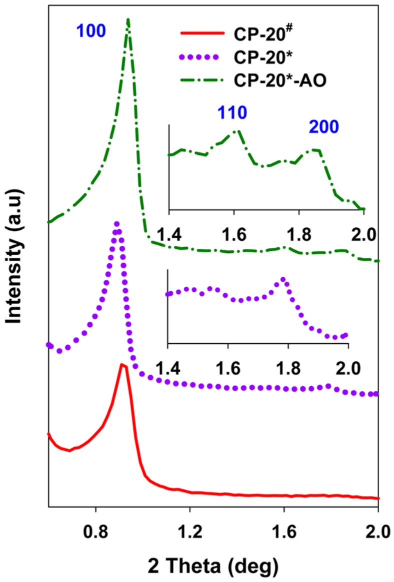

Figure 4. Small angle XRD patterns for the as-synthesized (CP-20$^{\#}$) and extracted (CP-20*) cyanopropyl-containing organosilica mesostructures, and for amidoxime-containing sample (CP-20*-AO).

The observed change in the XRD patterns with increasing loading of organic group correlates with the change in the shape of hysteresis loops of nitrogen adsorption isotherms shown in Figure 5 (curves 1 and 5), which can be associated with transition from hexagonal mesostructure to cage-like mesostructure. In the latter case, the observed delayed desorption and an abrupt closure of the hysteresis loop at the lower limit of relative pressure can be related to the smaller entrance to spherical cages. In the case of high organic loading (for instance, CP-40*) some disruption in the formation of ordered mesostructure can be occur, which can result in poorly ordered or even disordered mesostructure. Thus, the XRD patterns imply that there is an optimum concentration of organic groups to form highly ordered mesostructures. Synthesis of organosiliceous mesostructures with zirconia led to the structurally disordered samples. The small angle XRD patterns did not show characteristic peaks for those mesostructures (not shown here). It is not surprising that the samples obtained by using high percentage of CPS (40%) in addition to zirconia precursors are disordered because a structural deterioration may occur due to perturbations of the self-assembly process caused by high loading of precursors in addition to the structure-forming TEOS. TEM images of CP-20* and CP-20*-AO displayed in Figure 6 show clearly that the samples obtained for 20% of CPS in the synthesis gel are highly ordered.

N_2 Adsorption Properties. Nitrogen adsorption−desorption isotherms measured at −196 °C for CP-(X)*, CP-(X)*-AO (X = 10,20,40), Zr-CP-20*, and Zr-CP-20*-AO samples are shown in Figure 5 and Figure S5 in the Supporting Information. Adsorption parameters of the aforementioned samples such as the BET surface area, single-point pore volume, mesopore diameter, and micropore volume are summarized in

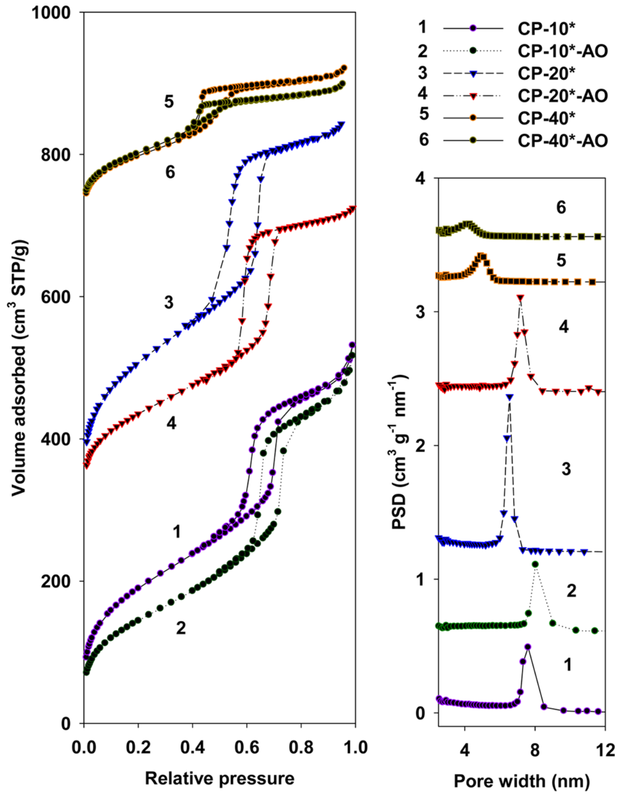

Figure 5. Nitrogen adsorption isotherms (left panel) and the corresponding PSD curves (right panel) for extracted (*) cyanopropyl and amidoxime-containing organosilica mesostructures; the isotherm curves 3&4 and 5&6 are shifted by 300 and 700 cm^3 STP/g, respectively, in relation to 1 and 2. The PSD curves 2, 3, 4, 5, and 6 are shifted by 0.6, 1.2, 2.4, 3.2, and 3.6 cm^3 g^{-1} nm^{-1}, respectively, in relation to curve 1.

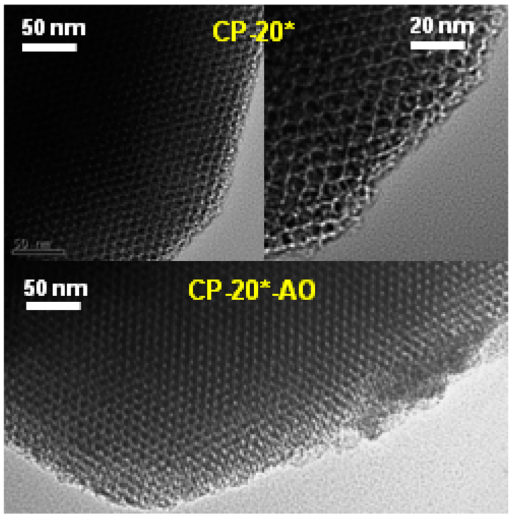

Figure 6. TEM images of the CP-20 * (top) and CP-20*-AO (bottom) samples.

Table 1. The CP-(*X*)* and CP-(*X*)*-AO (*X* = 10, 20) samples exhibit type IV isotherms with sharp capillary condensation-evaporation steps and distinct narrow H1 hysteresis loops starting at relative pressure of about 0.65−0.7. The sample synthesized with highest amount of CPS (CP-40*) features type (IV) isotherm with H2 hysteresis loop. The condensation step starts at relative pressure of about 0.6. The H2 hysteresis loop is characteristic for the cage-like or constricted mesopores; as indicated in the preceding section, it is possible that hexagonal structure changed to cagelike at high concentration of organic groups.

Nitrogen adsorption isotherms were used to obtain basic parameters such as the specific surface area, pore volume, and pore size, which are listed in Table 1. The pore diameters were evaluated by the KJS method.[32] The nitrogen uptake for CP-40* is smaller, indicating a decrease in the volume of mesopores. This behavior can be anticipated due to the geometrical constrictions associated with the accommodation of a large amount of cyanopropyl groups in the mesostructure. Similarly, all amidoxime-modified mesostructures exhibit type IV isotherms with H1/H2 hysteresis loops depending on the concentration of organic groups. Another exciting feature of amidoxime-modified mesostructures is the absence of any significant alternation of the isotherm shape due to modification. However, amidoximation causes a substantial decrease in the BET surface area, microporosity, and total pore volume as compared to the unmodified counterparts. Although, one can expect that the observed decrease in the aforementioned quantities can be caused by some structural collapse during amidoximation, the XRD patterns shown in Figure 4 and Figure S4 in the Supporting Information indicate that the modification conditions did not considerably alter the mesoporous ordering. The samples with incorporated zirconia show type IV isotherms with H1/H2 hysteresis loops. Their PSD curves are somewhat broader and bimodal (Figure S5 in the Supporting Information), indicating that the addition zirconia causes a significant perturbation of the self-assembly process; consequently, disordered composite samples are formed.

CO_2 Capture at Elevated Temperatures. The most of commercially available amines or amine-containing organosilica decompose upon thermal treatment beyond 120 °C and thus, it is difficult to apply them for CO_2 capture at elevated temperatures. The discussed above thermogravimetric data show that the amidoxime-modified silica mesostructures are stable in the temperature range of 400−550 °C. In this temperature range amidoxime groups do not decompose under neutral conditions due to strong C−C and C═N bonds. Thus, the amidoxime-modified organosilica materials can be attractive sorbents for CO_2 capture at the elevated temperatures, 100−150 °C. CO_2 sorption and desorption temperatures for amidoxime-modified samples were selected on the basis of the DTG curves. Therefore, the amidoxime-modified mesoporous organosilica materials intended for CO_2 capture were subjected to pretreatment in inert He gas up to 350 °C followed by preferential pulse CO_2 chemisorption at 60/120 °C and subsequently subjected to desorption by ramping temperature up to 350 °C. As can be seen from Figure 7, after thermal pretreatment of the sample, a steady stream (pulse) of CO_2 gas was flowing through the sample and it was immobilized on available active sites (−NH−OH and NH_2). Desorption of CO_2 was achieved by raising the temperature linearly with time in flowing inert carrier gas (He) through the sample. CO_2 sorption at 60/120 °C was measured as a function of temperature. The most of CO_2 captured at 60 and 120 °C was desorbed at 345 and 340 °C, respectively (Figures 8 and 9).

As can be seen from Figures 8 and 9, and Table 2, CO_2 sorption capacity can be enlarged by increasing the concentration of amidoxime groups. Regardless of CO_2

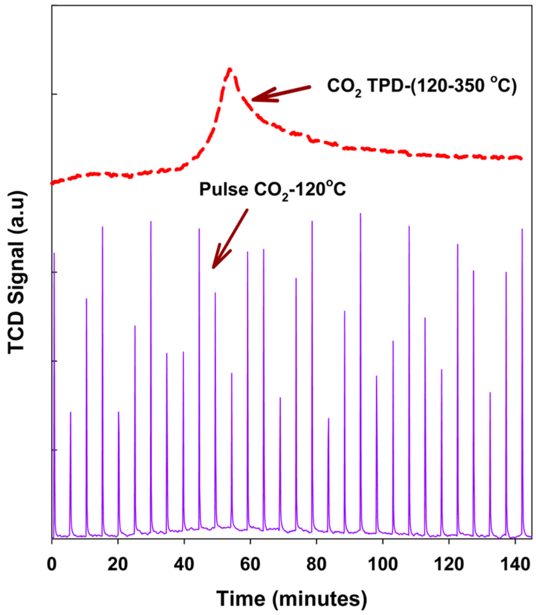

Figure 7. Pulse and CO_2 TPD profiles measured on the CP-20*-AO Sample.

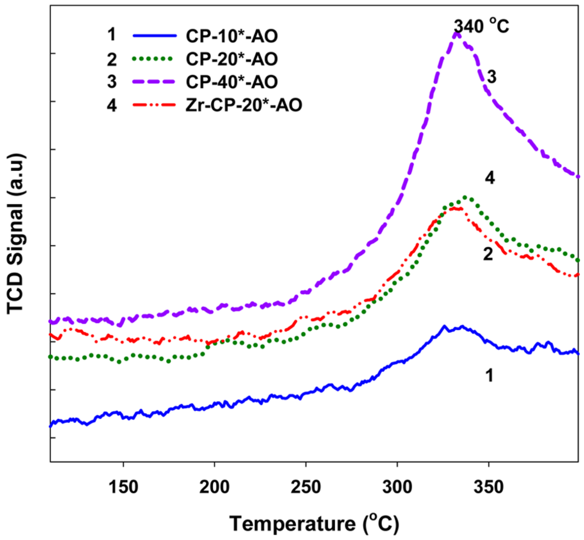

Figure 8. CO_2 TPD (pulse at 120 °C) profiles recorded for the CP-X*-AO and Zr-CP-20*-AO samples.

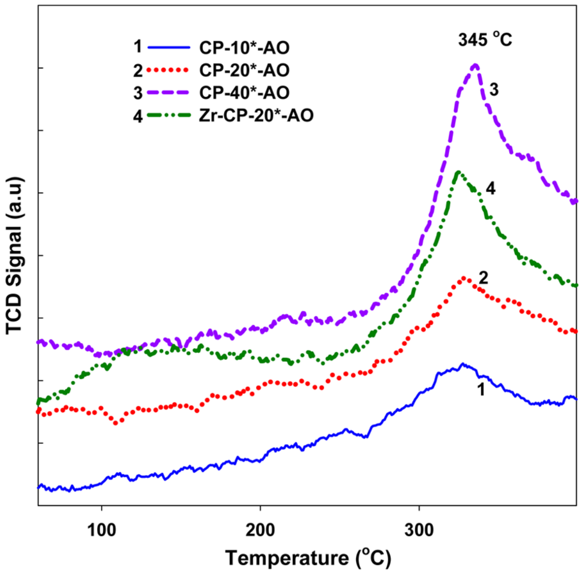

Figure 9. CO_2 TPD (pulse at 60 °C) profiles recorded for CP-X*-AO and Zr-CP-20*-AO samples.

Table 2. CO_2 Sorption Values at 60 and 120 °C for Amidoxime-Modified Organosilica Samples[a]

sample	max CO_2 sorption at 60 °C (mmol/g)	max CO_2 sorption at 120 °C (mmol/g)
CP-10*-AO	2.02	1.80
CP-20*-AO	2.67	2.49
CP-40*-AO	3.28	3.07
Zr-CP-20*-AO	2.79	2.53

[a] The amount of desorbed CO_2 was obtained by integration of the desorption profiles during TPD.

sorption at 60 or 120 °C, the sorption capacity decreased in the following order: CP-40*-AO> CP-20*-AO> CP-10*-AO. The CP-40*-AO sample showed the maximum CO_2 uptake of about 3.28 and 3.07 mmol/g at 60 and 120 °C, respectively. The amounts of thermodesorbed CO_2 that are listed in Table 2 are amazingly competitive as compared to the values reported in literature. For instance, the CO_2 sorption capacities reported for mesoporous alumina and alumina-supported metal oxides (Ca, Mg, Ce, Cu, Cr) at 120 °C by Cai and co-workers[37] did not exceed the value of 1.8 mmol/g. The CO_2 uptakes measured on a zeolite at 120 °C by Siriwardena and co-workers achieved the values of 0.7 and 1.2 mmol/g at 1 and 20 bar, respectively.[38] The CO_2 capacities measured on a MgO/Al_2O_3 composite sorbent[39] at 60 °C were equal to 0.97 and 1.36 mmol/g in the presence (13%) and absence (0%) of water vapor, respectively. The highest value of CO_2 uptake obtained for mesoporous isocyanurate-containing organosilica—alumina composites at 120 °C was about 2.2 mmol/g.[40]

A very high value of the CO_2 capacity reported here was possible because of synthesizing organosilica mesostructures with high loading of cyanopropyl groups, which were successfully converted to amidoxime groups having two active sites, −NH(OH) and $-NH_2$, per one ligand. A comparison of the CO_2 uptake of the amidoxime-modified organosilica mesostructures discussed in this work with the data recently reported for amidoxime compounds and amidoxime-grafted carbons and polymers,[20−22] our materials showed better performance. For instance, Zulfiqur and co-workers[20] reported CO_2 uptake at extremely high pressures (180 bar) and moderately low temperatures (43 and 70 °C), and achieved the maximum CO_2 uptake about of 1.64 and 2.71 mmol/g at 43 and 70 °C, respectively; note that higher CO_2 uptake at 70 °C is due to chemisorption, whereas physisorption dominates at 43 °C. However, our samples examined at atmospheric pressure and higher temperatures (60, 120 °C) showed higher CO_2 uptakes. The conditions tested in this work better reflect the industrial situation because fossil fuels-based power plants discharge flue gas at atmospheric pressure with low partial pressure of CO_2 in the temperature range of ∼100−150 °C.[41] Additional advantages of the samples studied are their excellent thermal stability up to 400 °C as compared to amine-containing solid sorbents, which decompose typically above 100 °C.[15−17] For instance, the amidoxime-modified mesoporous organosilica materials displayed a remarkable stability with no noticeable structural degradation during chemisorption (<300 °C) and desorption (<400 °C). Moreover, the chelating ability of amidoxime groups eliminates the oxidative degradation, which increases the lifetime of these sorbents and reduces the cost of the CO_2 capture process[18]

Although our expectation was to increase the CO_2 sorption capacity by incorporating zirconia into amidoxime-modified silica sorbent (Zr-CP-20*-AO), only a small increase in the CO_2 capacity was achieved as compared to that obtained for CP-20*-AO. If dissimilar active sites are present in a composite sorbent, desorption of CO_2 species occurs at different temperatures. It is possible that desorption of CO_2 from amidoxime-modified organosilica-zirconia composites could occur in a broader temperature range beyond 350 °C, which could not be studied by us because of possible decomposition of amidoxime groups.

There is an extensive literature on the mechanism of CO_2 interactions with amine groups (see for instance ref 42). It was shown earlier that under anhydrous conditions, one mole of CO_2 reacts with two moles of amine groups. The overall reaction between CO_2 with primary and secondary amines occurs through the carbomate formation:[42]

$$CO_2 + 2R_1R_2NH \rightarrow R_1R_2NH_2 + +R_1R_2NCO_2^-$$

where R_1 or R_2 denote H in the case of primary amines, and aryl/alkyl groups in the case of secondary amines. According to Dankwerts' zwitterion mechanism,[42] the above reaction involves the formation of a zwitterion intermediate by binding CO_2 to a single amine molecule followed by transfer of proton to another amine molecule

$$CO_2 + R_1R_2NH \rightarrow R_1R_2NH^+CO_2^-$$

$$R_1R_2NH^+CO_2^- + R_1R_2NH \rightarrow R_1R_2NH_2^+ + R_1R_2NCO_2^-$$

Amidoxime-modified mesoporous organosilica has primary amine (R-NH_2) and oxime (R−C═N−OH) groups (see Figure S1 in the Supporting Information). Hydrogen carbonate species can be formed between CO_2 and basic hydroxyl groups (see Figure S6 in the Supporting Information). Thus, N−OH groups can attract CO_2 to from bicarbonate structure.[23,42,43] However, hydrogen carbonate species can be decomposed at low temperatures[23,42,43] (above 100 °C). Therefore, the carbomate formation is a reasonable mechanism for interaction between CO_2 and primary amines present in amidoxime groups.

The formation of carbomate species requires breaking the N−H bond and trapping proton by another amine group. Since the reaction with CO_2 involves two nitrogen atoms in amine groups as reported by Hiyoshi et al.[43] and Prasetyanto group,[44] in order to form carbomate structure efficiently, two nitrogen atoms at close proximity are essential for effective binding (Figure 10). According to Dankwerts' mechanism, CO_2 chemisorption can occur with amine pairs very effectively,[42] whereas isolated amine groups are less prone for binding. Prasetyanto group used melamine trisilesquioxane bridged organosilica for CO_2 sorption and they showed possible mechanism for CO_2 activation via a cyclic carbomate formation.[44] On the basis of these studies, we believe that in the case of amidoxime-modified mesoporous organosilicas studied, there is a very favorable environment for CO_2 sorption, which is confirmed by high CO_2 sorption capacities on these sorbents at elevated temperatures (see Table 2).

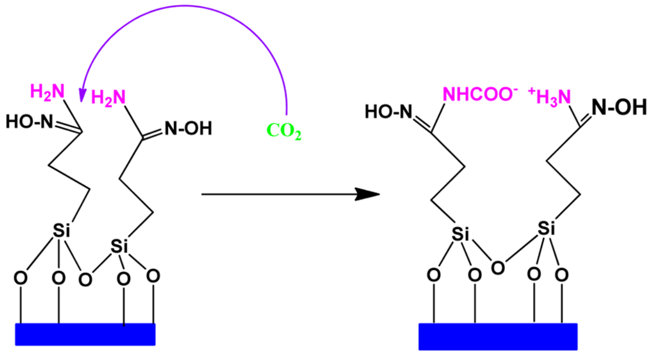

Figure 10. Systematic illustration of CO_2 binding on amidoxime-modified organosilica.

CO_2 Physisorption. The amidoxime-modified organosilica mesostructures were also examined for CO_2 adsorption at room temperature (25 °C). Adsorption isotherms for CO_2 measured on these sorbents and the cyanopropyl-containing counterparts up to 1 bar at 298 K are shown in Figure 11.

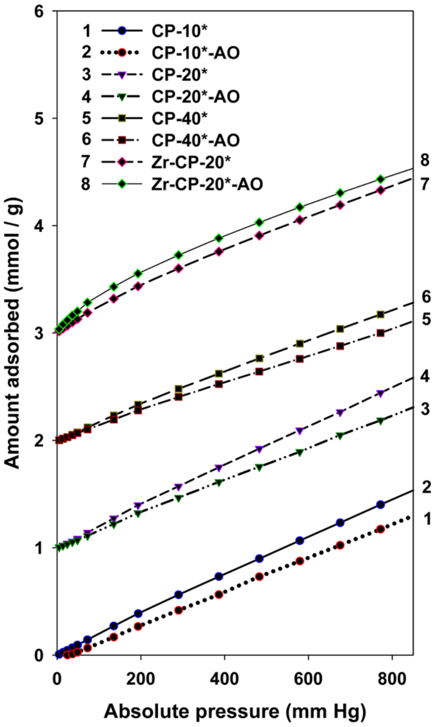

Figure 11. CO_2 adsorption isotherms at 25 °C measured on CP-(X)* and Zr-CP-20* and the corresponding amidoximated samples (X = 10, 20, 40). The isotherm curves 3 & 4, 5 & 6, and 7 & 8 are shifted by multiple values of 1 mmol/g from 1 & 2.

Interestingly, the cyanopropyl-containing ordered mesoporous organosilica samples CP-(X)* (X = 10, 20, 40) and Zr-CP-20* showed slightly higher CO_2 sorption capacitates than those obtained for the corresponding amidoxime-modified samples (see Table 3). It should be noted further that CP-20* exhibited the CO_2 uptake of about 1.79 mmol/g, whereas the corresponding capacity of CP-20*-AO was 1.45 mmol/g. Although sorption of CO_2 at 60 and 120 °C increased with increasing concentration of amidoxime groups in the samples (see Figure 12), an opposite trend is observed for CO_2 adsorption at 25 °C; the CP-40*-AO sample adsorbed 1.22

Table 3. CO_2 Adsorption Values at 25 °C for the Samples Studied

sample	S_{BET} (m^2/g)	max CO_2 adsorption at 1 bar (mmol/g)	max CO_2 adsorption ($\mu mol/m^2$)
CP-10*	698	1.67	2.39
CP-10*-AO	533	1.46	2.74
CP-20*	771	1.79	2.32
CP-20*-AO	500	1.45	2.90
CP-40*	363	1.31	3.60
CP-40*-AO	257	1.22	4.75
Zr-CP-20*	599	1.57	2.62
Zr-CP-20*-AO	585	1.55	2.65

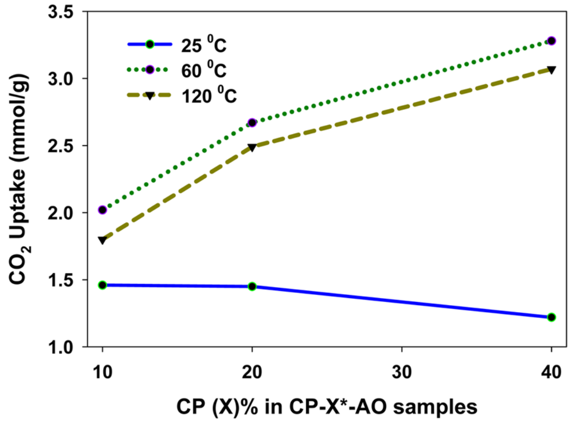

Figure 12. CO_2 uptake change with the percentage of the CPS used in the synthesis of CP-X*-AO samples at different temperatures.

mmol/g of CO_2, which is lower than that obtained for CP-20*-AO. Thus, it can be concluded that CO_2 sorption at ambient temperatures is mainly governed through physisorption mechanism, which is mainly affected by microporosity and surface area; the basic nature of organic groups is essential in chemisorption, which takes place at higher temperatures. It is also noteworthy to observe the higher CO_2 uptake for the sample with higher microporosity. This indicates the importance of fine pores in CO_2 adsorption at 25 °C and 1 bar. It was shown earlier that the CO_2 adsorption under ambient conditions is mainly determined by the volume of ultramicropores[45] (pores below 0.7 nm).

CONCLUSIONS

A series of amidoxime-functionalized ordered mesoporous organosilicas was obtained via amidoximation of cyanopropyl-containing organosilica mesostructures. These samples were shown to be fairly good sorbents for CO_2 capture at 25 °C through the physisorption mechanism. In contrast, the amidoxime-modified organosilica mesostructures were shown to be superior sorbents for CO_2 capture at 60 and 120 °C, achieving capacity above 3 mmol/g. These materials can be regenerated at the temperature range of 300−340 °C. Higher CO_2 uptake at 60 and 120 °C was obtained for materials with higher concentration of amidoxime groups. The importance of these groups for CO_2 capture at elevated temperatures is evidenced by pulse CO_2 chemisorption and TPD measurements. High adsorption capacity at elevated temperatures, preferential selectivity, low cost of the amidoxime-containing organosilica sorbent along with chemical and mechanical stability of amidoxime groups makes it a noticeable material for CO_2 capture as compared to the commercially available liquid ethanolamine (EA).

ASSOCIATED CONTENT

Ⓢ Supporting Information

Two schemes illustrating the conversion of cyanopropyl groups to amidoxime groups and the interaction of CO_2 with amidoxime groups, and four figures with thermogravimetric, small-angle XRD, and nitrogen adsorption data for the samples studied. This material is available free of charge via the Internet at http://pubs.acs.org/.

AUTHOR INFORMATION

Corresponding Author

*E-mail: jaroniec@kent.edu. Phone: 330-672-3790. Fax: 330-672-3816.

Notes

The authors declare no competing financial interest.

ACKNOWLEDGMENTS

The TEM data were obtained at the (cryo) TEM facility at the Liquid Crystal Institute, Kent State University, supported by the Ohio Research Scholars Program Research Cluster on Surfaces in Advanced Materials. The authors thank Dr. Min Gao and Michal Marszewski for technical support with the TEM experiments. Thanks to Dr. Mahinda Gangoda for technical support with the NMR measurements.

REFERENCES

(1) Davis, J.; Rochelle, G. Thermal Degradation of Monoethanolamine at Stripper Conditions. *Energy Procedia* **2009**, *1*, 327−333.

(2) Haszeldine, R. S. Carbon Capture and Storage: How Green Can Black Be? *Science* **2009**, *325*, 1647−1652.

(3) Voss, R.; Thomas, A.; Antonietti, M.; Ozin, G. A. Synthesis and Characterization of Highly Amine Functionalized Mesoporous Organosilicas by an "all-in-one" Approach. *J. Mater. Chem.* **2006**, *15*, 4010−4014.

(4) Van der Voort, P.; Vercaemst, C.; Schaubroeck, D.; Verpoort, F. Ordered Mesoporous Materials at the Beginning of the Third Millennium: New Strategies to Create Hybrid and Non-Siliceous. *Phys. Chem. Chem. Phys.* **2008**, *10*, 347−360.

(5) Hoffmann, F.; Cornelius, M.; Morell, J.; Froba, M. Silica-Based Mesoporous Organic-Inorganic Hybrid Materials. *Angew. Chem.* **2006**, *45*, 3216−3251.

(6) Hunks, W. J.; Ozin, G. A. Challenges and Advances in the Chemistry of Periodic Mesoporous Organosilicas (PMOs). *J. Mater. Chem.* **2005**, *15*, 3716−3724.

(7) Canck, E. D.; Ascoop, I.; Sayari, A.; Van der Voort, P. Periodic Mesoporous Organosilicas Functionalized with a Wide Variety of Amines for CO_2 Adsorption. *Phys. Chem. Chem. Phys.* **2013**, *15*, 9792−9799.

(8) Knowles, G. P.; Delaney, S. W.; Chaffee, A. L. Amine-Functionalised Mesoporous Silicas as CO_2 adsorbents. *Surf. Sci.* **2005**, *156*, 887−896.

(9) Knowles, G. P.; Graham, J. V.; Delaney, S. W.; Chaffee, A. L. Aminopropyl-Functionalized Mesoporous Silicas as CO_2 adsorbents. *Catal. Fuel Process. Technol.* **2005**, *86*, 1435−1448.

(10) Knowles, G. P.; Delaney, S. W.; Chaffee, A. L. Diethylenetriamine[propyl(silyl)]-Functionalized (DT) Mesoporous Silicas as CO_2 Adsorbents. *Ind. Eng. Chem. Res.* **2006**, *45*, 2626−2633.

(11) Hiyoshi, N.; Yogo, K.; Yashima, T. Adsorption Characteristics of Carbon Dioxide on Organically Functionalized SBA-15. *Microporous Mesoporous Mater.* **2005**, *84*, 357−365.

(12) Zelenak, V.; Halamova, D.; Gaberova, L.; Bloch, E.; Llewellyn, P. Amine-Modified SBA-12 Mesoporous Silica for Carbon Dioxide Capture: Effect of Amine Basicity on Sorption Properties. *Microporous Mesoporous Mater.* **2008**, *116*, 358−364.

(13) Harlick, P. J. E.; Sayari, A. Applications of Pore-Expanded Mesoporous Silicas. 3- Triamine Silane Grafting for Enhanced CO_2 Adsorption. *Ind. Eng. Chem. Res.* **2006**, *45*, 3248−3255.

(14) Arnold, D. S.; Barrett, D. A.; Isom, R. H. CO_2 Can Be Produced from Flue Gas. *Oil Gas J.* **1982**, *80*, 130−136.

(15) Sayari, A.; Gorji, A. H.; Yang, Y. CO_2-Induced Degradation of Amine-Containing Adsorbents: Reaction Products and Pathways. *J. Am. Chem. Soc.* **2012**, *134*, 13834−13842.

(16) Gorji, A. H.; Belmabkhout, Y.; Sayari, A. Degradation of Amine-Supported CO_2 Adsorbents in the Presence of Oxygen-Containing gases. *Microporous Mesoporous Mater.* **2011**, *145*, 146−149.

(17) Belmabkhout, Y.; Sayari, A. Effect of Pore Expansion and Amine Functionalization of Mesoporous Silica on CO_2 Adsorption over a Wide Range of Conditions. *Adsorption* **2009**, *15*, 318−328.

(18) Yu, C. H.; Huang, C. H.; Tan, C. S. A Review of CO_2 Capture by Absorption and Adsorption. *Aerosol Air Qual. Res.* **2012**, *12*, 745−769.

(19) Rochelle, G. T. Amine Scrubbing for CO_2 Capture. *Science* **2009**, *325*, 1652−1654.

(20) Zulfiqar, C.; Karadas, F.; Park, J.; Deniz, E.; Stucky, G. D.; Jung, Y. Amidoximes: Promising Candidates for CO_2 Capture. *Energy Environ. Sci.* **2011**, *4*, 4528−4531.

(21) Mahurin, S. M.; Gorka, J.; Nelson, K. M.; Mayes, R. T.; Dai, S. Enhanced CO_2/N_2 Selectivity in Amidoxime-Modified Porous Carbon. *Carbon* **2014**, *67*, 457−464.

(22) Patel, H. A.; Yavuz, C. T. Noninvasive Functionalization of Polymers of Intrinsic Microporosity for enhanced CO_2 capture. *Chem. Commun.* **2012**, *48*, 9989−9991.

(23) Baeza, B. B.; Ramos, I. R.; Ruiz, A. G. Interaction of Carbon Dioxide with the Surface of Zirconia Polymorphs. *Langmuir* **1998**, *14*, 3556−3564.

(24) Hornebecq, V.; Knofel, C.; Boulet, P.; Kuchta, B.; Llewellyn, P. L. Adsorption of Carbon Dioxide on Mesoporous Zirconia: Microcalorimetric Measurements, Adsorption Isotherms Modeling and Density-Functional Theory Calculations. *J. Phys. Chem. C* **2011**, *115*, 10097−10103.

(25) Pokrovski, K.; Jung, K. T.; Bell, A. T. Investigation of CO and CO_2 Adsorption on Tetragonal and Monoclinic Zirconia. *Langmuir* **2001**, *17*, 4297−4303.

(26) Na, C. K.; Park, H. J.; Kim, B. G. Optimal Amidoximation Conditions of Acrylonitrile Grafted onto Polypropylene by Photoirradiation-Induced Graft Polymerization. *J. Appl. Polym. Sci.* **2012**, *125*, 776−785.

(27) Gorka, J.; Mayes, R. T.; Baggetto, L.; Veith, G. M.; Dai, S. Sonochemical Functionalization of Mesoporous Carbon for Uranium Extraction from Seawater. *J. Mater. Chem. A* **2013**, *1*, 3016−3026.

(28) Sekiguchi, K.; Saito, K.; Konishi, S.; Furusaki, S. Effect of Seawater Temperature on Uranium Recovery from Seawater Using Amidoxime Adsorbent. *Ind. Eng. Chem. Res.* **1994**, *33*, 662−666.

(29) Choia, S. H.; Nhob, Y. C. Adsorption of UO_2^{2+} by Polyethylene Adsorbents with Amidoxime, Carboxyl, and Amidoxime/Carboxyl group. *Radiat. Phys. Chem.* **2000**, *57*, 187−193.

(30) Escoto, J. L.V.; Carboni, M.; Abney, C. W.; Dekrafft, K. E.; Lin, W. Organo-Functionalized Mesoporous Silicas for Efficient Uranium Extraction. *Microporous Mesoporous Mater.* **2013**, *180*, 22−31.

(31) Zhao, D.; Huo, Q.; Feng, J.; Chmelka, B. F.; Stucky, G. D. Nonionic Triblock and Star Diblock Copolymer and Oligomeric Surfactant Syntheses of Highly Ordered, Hydrothermally Stable, Mesoporous Silica Structures. *J. Am. Chem. Soc.* **1998**, *120*, 6024−6036.

(32) Kruk, M.; Jaroniec, M.; Sayari, A. Application of Large Pore MCM-41 Molecular Sieves to Improve Pore Size Analysis Using Nitrogen Adsorption Measurements. *Langmuir.* **1997**, *13*, 6267−6273.

(33) Alauzun, J.; Mehdi, A.; Reye, C.; Corriu, R. J. P. Direct Synthesis of Bifunctional Mesoporous Organosilicas Containing Chelating Groups in the Framework and Reactive Functional Groups in the Channel Pores. *J. Mater. Chem.* **2007**, *17*, 349−356.

(34) Boullanger, A.; Gracy, G.; Bibent, N.; Vinot, S. D.; Clément, S.; Mehdi, A. From an Octakis(3- cyanopropyl)silsesquioxane Building Block to a Highly COOH-Functionalized Hybrid Organic−Inorganic Material. *Eur. J. Inorg. Chem.* **2012**, 143−150.

(35) Kobuke, Y.; Tanaka, H.; Ogoshi, H. Imidedioxime as a Significant Component in So-Called Amidoxime Resin for Uranyl Adsorption from Seawater. *Polymer J.* **1990**, *22*, 179−182.

(36) Egawa, H.; Kabay, N.; Shuto, T.; Jyo, A. Recovery of Uranium from Seawater. Preparation and Characterization of Lightly Crosslinked Highly Porous Chelating Resins Containing Amidoxime groups. *J. Appl. Polym. Sci.* **1992**, *46*, 129−142.

(37) Cai, W.; Yu, J.; Anand, C.; Vinu, A.; Jaroniec, M. Facile Synthesis of Ordered Mesoporous Alumina and Alumina-Supported Metal Oxides with Tailored Adsorption and Framework Properties. *J. Mater. Chem.* **2011**, *23*, 1147−1157.

(38) Siriwardena, R. V.; Shen, M. S.; Fisher, E. P. Adsorption of CO_2 on Zeolites at Moderate Temperatures. *Energy Fuels* **2005**, *19*, 1153−1159.

(39) Li, L.; Wen, X.; Fu, X.; Wang, F.; Zhao, N.; Xiao, F.; Wei, W.; Sun, Y. MgO/Al_2O_3 Sorbent for CO_2 Capture. *Energy Fuels* **2010**, *24*, 5773−5780.

(40) Gunathilake, C.; Gangoda, M.; Jaroniec, M. Mesoporous Isocyanurate-Containing Organosilica−Alumina Composites and Their Thermal Treatment in Nitrogen for Carbon Dioxide Sorption at Elevated Temperatures. *J. Mater. Chem. A* **2013**, *1*, 8244−8252.

(41) Samanta, A.; Zhao, A.; Shimizu, G. K. H.; Sarkar, P.; Gupta, R. Post-Combustion CO_2 Capture Using Solid Sorbents: A Review. *J. Am. Chem. Soc.* **2012**, *51*, 1438−1463.

(42) Dankwerts, P. V. The Reaction of CO_2 with Ethanolamines. *Chem. Eng. Sci.* **1979**, *34*, 443−445.

(43) Hiyoshi, N.; Yogo, K.; Yashima, T. Adsorption characteristics of carbon dioxide on organically functionalized SBA-15. *Microporous Mesoporous Mater.* **2005**, *84*, 357−365.

(44) Prasetyanto, E. A.; Ansari, M. B.; Min, B. H.; Park, S. E. Melamine Tri-Silsesquioxane Bridged Periodic Mesoporous Organosilica as an Efficient Metal-Free Catalyst for CO_2 Activation. *Catal. Today* **2010**, *158*, 252−257.

(45) Wickramaratne, N. P.; Jaroniec, M. Importance of Small Micropores in CO_2 Capture by Phenolic Resin-Based Activated Carbon Spheres. *J. Mater. Chem. A* **2013**, *1*, 112−116.